



January 30, 2013  
NRC:13:007

Document Control Desk  
U.S. Nuclear Regulatory Commission  
Washington, D.C. 20555-0001

**Response to U.S. EPR Design Certification Application RAI No. 349, Supplement 21**

Ref. 1: E-mail, Getachew Tesfaye (NRC) to Ronda Pederson, et al (AREVA NP Inc.), "U.S. EPR Design Certification Application RAI No. 349 (4164, 4165), FSAR Ch. 19 OPEN ITEM," January 8, 2010.

Ref. 2: E-mail, Dennis Williford (AREVA NP Inc.) to Getachew Tesfaye (NRC), "Response to U.S. EPR Design Certification Application RAI No. 349, FSAR Ch. 19 OPEN ITEM, Supplement 20," November 27, 2012.

In Reference 1, the NRC provided a request for additional information (RAI) regarding the U.S. EPR design certification application. Reference 2 provided a schedule for the two remaining questions, and a history of the prior supplemental responses.

Enclosed is a technically correct and complete final response to the two remaining questions of RAI 349. The following table indicates the respective pages in the enclosed response that contain AREVA NP Inc.'s (AREVA NP) final response to the subject questions.

Question #	Start Page	End Page
RAI 349 — 19-334	2	18
RAI 349 — 19-335	19	30

AREVA NP considers some of the material contained in the attached response to be proprietary. As required by 10 CFR 2.390(b), an affidavit is attached to support the withholding of the information from public disclosure. Proprietary and non-proprietary versions of the enclosure to this letter are provided.

This concludes the formal AREVA NP response to RAI 349, and there are no questions from this RAI for which AREVA NP has not provided responses.

AREVA NP is in the process of updating the source term calculations for the Modular Accident Analysis Program (MAAP), which may have a minor impact on the source term results presented in the response to Question 19-335. The conclusion of the response, that MAAP4 analyses are in strong agreement with MELCOR for the first 24 hours, is not expected to be impacted, and AREVA NP is not anticipating the need for a revision to RAI 349, Question 19-335.

*DOTT  
MIRO*

If you have any questions related to this submittal, please contact Len Gucwa by telephone at (434) 832-3466, or by e-mail at [Len.Gucwa.ext@areva.com](mailto:Len.Gucwa.ext@areva.com).

Sincerely,

A handwritten signature in black ink, appearing to read 'Pedro Salas', is written over a large, horizontal, scribbled-out line.

Pedro Salas, Director  
Regulatory Affairs  
AREVA NP Inc.

Enclosures

cc: A. M. Snyder  
Docket No. 52-020

AFFIDAVIT

COMMONWEALTH OF VIRGINIA            )  
  ) ss.  
COUNTY OF CAMPBELL                 )

1. My name is Gayle F. Elliott. I am Manager, Product Licensing, for AREVA NP Inc. (AREVA NP) and as such I am authorized to execute this Affidavit.

2. I am familiar with the criteria applied by AREVA NP to determine whether certain AREVA NP information is proprietary. I am familiar with the policies established by AREVA NP to ensure the proper application of these criteria.

3. I am familiar with the AREVA NP information contained in the "Response to U.S. EPR Design Certification Application RAI No. 349, Supplement 21," and referred to herein as "Document." Information contained in this Document has been classified by AREVA NP as proprietary in accordance with the policies established by AREVA NP for the control and protection of proprietary and confidential information.

4. This Document contains information of a proprietary and confidential nature and is of the type customarily held in confidence by AREVA NP and not made available to the public. Based on my experience, I am aware that other companies regard information of the kind contained in this Document as proprietary and confidential.

5. This Document has been made available to the U.S. Nuclear Regulatory Commission in confidence with the request that the information contained in this Document be withheld from public disclosure. The request for withholding of proprietary information is made in accordance with 10 CFR 2.390. The information for which withholding from disclosure is

requested qualifies under 10 CFR 2.390(a)(4) "Trade secrets and commercial or financial information":

6. The following criteria are customarily applied by AREVA NP to determine whether information should be classified as proprietary:

- (a) The information reveals details of AREVA NP's research and development plans and programs or their results.
- (b) Use of the information by a competitor would permit the competitor to significantly reduce its expenditures, in time or resources, to design, produce, or market a similar product or service.
- (c) The information includes test data or analytical techniques concerning a process, methodology, or component, the application of which results in a competitive advantage for AREVA NP.
- (d) The information reveals certain distinguishing aspects of a process, methodology, or component, the exclusive use of which provides a competitive advantage for AREVA NP in product optimization or marketability.
- (e) The information is vital to a competitive advantage held by AREVA NP, would be helpful to competitors to AREVA NP, and would likely cause substantial harm to the competitive position of AREVA NP.

The information in the Document is considered proprietary for the reasons set forth in paragraphs 6(b) and 6(c) above.

7. In accordance with AREVA NP's policies governing the protection and control of information, proprietary information contained in this Document has been made available, on a limited basis, to others outside AREVA NP only as required and under suitable agreement providing for nondisclosure and limited use of the information.

8. AREVA NP policy requires that proprietary information be kept in a secured file or area and distributed on a need-to-know basis.

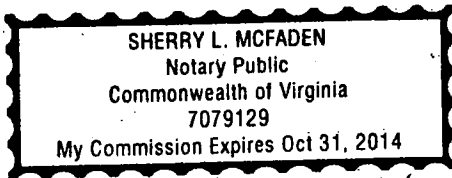
9. The foregoing statements are true and correct to the best of my knowledge, information, and belief.

A large, stylized handwritten signature in black ink, appearing to be 'A. R. H.', written over a horizontal line.

SUBSCRIBED before me this 30<sup>th</sup>  
day of January 2013.

A handwritten signature in black ink, appearing to be 'Sherry L. McFaden', written over a horizontal line.

Sherry L. McFaden  
NOTARY PUBLIC, COMMONWEALTH OF VIRGINIA  
MY COMMISSION EXPIRES: 10/31/2014  
Reg. #7079129



**Response to**

**Request for Additional Information No. 349, Supplement 21**

**01/26/2010**

**U. S. EPR Standard Design Certification**

**AREVA NP Inc.**

**Docket No. 52-020**

**SRP Section: 19 - Probabilistic Risk Assessment and Severe Accident Evaluation**

**Application Section: FSAR Chapter 19**

**QUESTIONS for PRA Licensing, Operations Support and Maintenance Branch 2  
(ESBWR/ABWR Projects) (SPLB)**

**Question 19-334:**

## OPEN ITEM

Follow-up to RAI 133, Question 19-230

In general, large phenomenological uncertainties are associated with the pre-mixing, detonation and propagation phases fuel-coolant interactions and the resulting energetics from steam explosions. These phenomenological uncertainties are, to some extent, reflected in the differences in the models and computer codes that are currently available worldwide.

In the pre-mixing phase, computer code differences include those affecting the modeling of fuel jet fragmentation and flow regime transition, among others. In the TEXAS and PH-ALPHA computer codes, the concept of leading edge jet breakup is used. On the other hand, the IKEMIX computer code used by the applicant is based on a continuous jet fragmentation concept. The RAI response claims that the leading edge break-up model results in more fuel mass participating in the pre-mixing process.

In addition, TEXAS and PM-ALPHA codes are based on the conceptualization of churn flow, while the IKEMIX code assumes a combination of bubbly and droplet flow. These differences affect the quantity of fuel that is in contact with the coolant, and it is expected to be higher for the TEXAS and PM-ALPHA codes, and affects the degree of void generation.

Therefore, given the uncertainties in the phenomenological representation of the premixing and propagation phases of steam explosions, the quantifications of the steam explosion-induced loads need to reflect these uncertainties. The documented uncertainty analysis that was performed by the applicant does not consider the larger loads that are envisioned using models such as TEXAS and PM/ALPHA/ESPROSE.

Furthermore, given the results of the recent staff confirmatory calculations using MELCOR, it has been noted that there is a potential for a delayed relocation of some of the core debris into the reactor pit, after the reactor pit plug melt-through. Therefore, the frequency of accidents where steam explosions are conceivable cannot be limited only to those involving high reactor coolant system pressure and creep-induced failure of the hot-leg nozzles. The majority of accidents in U.S. EPR result with melt cooling on the spreading compartment; therefore, any delayed release of core debris from the RPV into the reactor pit (i.e., after pit plug failure) could result in energetic fuel-coolant-interactions.

- a) Please revise the ex-vessel steam explosion analysis to reflect the potential impact of phenomenological uncertainties, especially, during the pre-mixing phase of a steam explosion.
- b) In addition, please discuss the consequences of steam explosions from delayed relocation of core debris from the reactor vessel (following pit plug melt-through) on the structural integrity of the pit, transfer channel, the spreading area (including the debris cooling structures), and the containment.

**Response to Question 19-334****Response to Question 19-334, Part a:**

The boundary conditions for the parameters considered to be the most critical for loads from ex-vessel steam explosion have been documented in the RAI 133, Supplement 6, "Response to Question 19-230(b)." The purpose of this RAI response is to provide additional clarification on the following aspects of the uncertainty analysis used for the U.S. EPR plant ex-vessel steam explosion:

- Address more comprehensively the phenomenological uncertainty related to the premixing stage, including the one related to the methodology used.
- Demonstrate that the blast correlation used in the uncertainty analysis has been benchmarked against deterministic codes. This is to gain confidence that the parametric correlation is capable of predicting the pressure loads calculated deterministically with the appropriate initial conditions.
- Justify that the efficiency (conversion ratio) range used in the uncertainty analysis is sufficient and adequate for the U.S. EPR initial conditions.

**1. Phenomenological Uncertainties During The Premixing Phase**

According to Reference 1 there are two distinct methodologies used in premixing codes that model jet fragmentation; the Kelvin-Helmholtz and the Taylor correlations. The code IKEJET/IKEMIX used to support the analysis presented in response to RAI 133, Question 19-230 models the Kelvin-Helmholtz correlation. To gain confidence in the results presented in the initial RAI response it is proposed in the present analysis to use the alternate method with a Taylor correlation. This approach is believed to cover all aspects of modeling uncertainties related to the premixed mass.

A number of parameters are unchanged compared to the initial calculation of premixed mass as they describe the specific scenario studied. These parameters are: melt composition and densities, water pool depth and jet diameter.

The other parameters are either modified or newly added to model different parametric uncertainties than previously presented. The parametric uncertainties used are based on the analysis presented in Reference 2. This analysis was chosen because it is an alternate method to the premixed model used in IKEMIX.

**Simplified Correlation for the Premixed Mass Uncertainty Calculation:**

A simplified approach to calculate the premixed mass was adopted to model the uncertainties of the premixed mass. The premixed mass is taken as a fraction of the total melt mass flowing from the reactor pressure vessel (RPV) break into the water pool during the period preceding triggering.

$$M = mass\ flow [kg / s] * f_B * T_{setling} [s] \quad \text{(Equation 1)}$$

Where:

$M[kg]$  is the premixed mass.

$mass\ flow[kg/s]$  is the mass flow rate of the melt through the RPV break.

$f_B$  is the fraction of the melt jet column participating in the premixing.

$T_{setling}[s]$  is the period of time necessary for the melt droplets resulting from the jet break up to settle at the bottom of the water pool.

The following simplifying assumptions are made in this case:

- The jet velocity is constant along the corium column and is equal to the velocity at the surface of the pool.
- Triggering is assumed to occur when the fragmented melt droplets settle at the bottom of the water pool. The settling time  $T_{setling}$  is then calculated as the ratio of the settling velocity  $V_{Setling}$  and the water pool height  $H$ . The settling velocity of the droplets is typically smaller than the velocity of the leading edge, allowing the melt to be added to the premixing region for a longer period of time.
- The lateral velocity of the melt droplets is neglected. This is conservative as all the melt droplets are contained in the premixing region.

$$M = \left( V_j [m/s] * \rho [kg/m^3] * \frac{(\pi D_{jet}^2)}{4} [m^2] \right) * f_B * \left( \frac{H}{V_{Setling}} [s] \right) \quad (\text{Equation 2})$$

Where:

$V_j [m/s]$  is the corium jet velocity at the water pool surface.

$\rho [kg/m^3]$  is the melt density.

$D_{jet} [m]$  is the corium jet diameter.

The fraction  $f_B$  of the melt jet column participating in the premixing was calculated based on the jet breakup length. The jet breakup length was calculated using a Taylor-type correlation. This correlation is in agreement with experimental observations for low-velocity jets according to References 2 and 3. The low velocity resulting from short free fall height is typical of PWR scenarios. Note that the calculated jet velocities in the case of the U.S. EPR

design are in the low range of Reference 2 for the lateral leak and about the same for the central leak.

The uncertainty distributions for the parameters used were selected when adequate from Reference 2. The experimental conditions described in Reference 2 are similar to the scenarios considered in the U.S. EPR plant ex-vessel steam explosion scenarios. The premixing model in Reference 2 was also based on the Taylor correlation.

Parametric Uncertainties Used in the Premixing Mass Calculation:

Revised or newly added parameters are described for the two scenarios analyzed in RAI 133, Supplement 6, "Response to Question 19-230; Ex-vessel Steam Explosion following Central and Lateral Leaks of the Reactor RPV."

Water Pool Depth (m) Unchanged:

The water pool depth for the lateral leak scenario is [ ] m and for the central leak scenario [ ] m.

Melt Density (m) Unchanged:

The density for a metallic melt is taken as [ ] (kg/m<sup>3</sup>) and for a mixed melt (metallic and oxidic) is assumed to be [ ] (kg/m<sup>3</sup>).

Jet Diameter (m) Unchanged:

The jet diameter is taken to be equal to the breach diameter. The same breach diameter ranges are used as in other parts of the U.S. EPR design certification Level 2 PRA. The bounding range used for the central leak is between [ ] cm while the range for the lateral leak is between [ ] cm and [ ] cm. For both cases uniform distributions have been used.

Jet Velocity (m/s):

The distribution from Table 1 of Reference 2 was used. This distribution is adapted to the central leak scenario as the maximum jet velocity calculated from the geometry of the melt in the RPV at the time of failure is [ ]. However, for the lateral RPV failure scenario the maximum calculated velocity is [ ] because of the lower depth of melt above the breach location. Therefore, the distribution from Reference 2 is shifted toward a lower range for the lateral leak scenario that is better representative of this case. Figure 19-334-1 shows the jet velocity distribution.

Droplets Settling Time (s):

The droplets settling time is calculated as the ratio of the water pool height, which is different for the lateral and the central leaks and the settling velocity. The correlation used is identical to Equation 6 of Reference 4.

$$T_{\text{settling}} = \frac{H}{V_{\text{Settling}}} \quad (\text{Equation 3})$$

The settling time represents the time period from the formation of melt droplets until they reach the bottom of the pool. For conservatism it is assumed that the droplets formation (from breakup) starts at the surface of the water pool as soon as the molten jet penetrates the water pool.

#### Melt Droplet Settling Velocity (m/s):

The settling velocity is taken as Equation 7 of Reference 4. A number of parameters used for the calculation of the settling velocity are sampled from uncertainty distributions, the void fraction, and the melt droplets diameter. These distributions are described below.

$$V_s = \sqrt{\frac{4}{3C_f}} * \sqrt{\frac{\rho_M - \rho_C}{\rho_C}} * \sqrt{g} * \sqrt{D_p}$$

$$\rho_C = \alpha * \rho_G + (1 - \alpha) * \rho_L \quad (\text{Equation 4})$$

Where:

$\alpha$  = void fraction sampled from a distribution.

$\rho_G$  = vapor in pool @ (1 bar) saturation 0.59 (kg/m<sup>3</sup>).

$\rho_L$  = water in pool @ (1 bar) saturation 958.63 (kg/m<sup>3</sup>).

$D_p$  = droplet diameter sampled from a distribution.

$C_p$  = 0.44 drag coefficient Newton regime from Reference 4.

$g$  = gravitational acceleration 9.8 m/s<sup>2</sup>.

#### Droplet Size (mm):

The continuous distribution presented in Table 1 of Reference 2 was used, since it was considered to be better adapted to the physical mechanism of droplets formation. A sensitivity run was performed with the droplet discrete distribution used in PM-ALPHA as documented in Table 13 of Reference 5 for the ex-vessel case (80 percent with 15 mm diameter size and 20 percent with 3 mm diameter size). The sensitivity run showed a decrease of approximately 0.4 percent in the containment failure probability compared to the base case that used the custom distribution described below. Since the droplets diameter distribution has a minimal impact on the premixed mass, the continuous distribution is used in the present analysis. Figure 19-334-2 shows the droplet size distribution.

Void Fraction:

The void fraction is sampled from a uniform distribution with a range between 0.3 and 0.7. This range is taken from Table 1 of Reference 2 and considered justified given the saturated water condition (water in the pit is subsequent to an induced hot leg rupture) seen in the two scenarios considered. Figure 19-334-3 shows the void fraction distribution.

Jet Breakup Fraction  $f_B$ :

The fraction of the total mass of corium in the water pool that participates in the premixing phase is taken as the jet breakup fraction. As noted, although this is a simplification for the uncertainty analysis, conservative assumptions are made on a number of parameters.

The definition of the breakup fraction is taken from Equation 4.1 of Reference 3 as:

$$f_B = 1 - \left( \frac{D_{jb}^2}{D_{ji}^2} \right) \quad \text{(Equation 5)}$$

Using the assumption that the jet cross section linearly decreases along the water pool depth  $H$ , then:

$$\frac{Lbrk - H}{Lbrk} = \frac{D_{jb}^2}{D_{ji}^2} \quad \text{(Equation 6)}$$

Therefore,

$$f_B = \frac{H}{Lbrk} \quad \text{(Equation 7)}$$

Where:

$Lbrk$ : is the hypothetical jet breakup length (m)

$H$ : the pool depth (m)

$D_{jb}$ : jet diameter at the bottom of the pool (m)

$D_{ji}$ : jet diameter at the (inlet) water pool surface (m)

Sensitivity on the constant jet diameter assumption was run. If the jet diameter were assumed to decrease linearly with the pool depth instead of the jet cross section then Equation 4.6 of Reference 3 should be used in this case:

$$f_B = (1 - (1 - X)^2) * X^{1/2} \quad \text{(Equation 9)}$$

Where:

$$X = \frac{H}{Lbrk}$$

Note:

Equation 9 was not used to calculate the jet breakup fraction because it resulted in slightly lower premixed masses than Equation 7 used in this analysis.

Jet Breakup Length (m):

The hypothetical jet breakup length  $Lbrk$  is calculated using the Taylor correlation:

$$\frac{Lbrk}{Dji} = CN_p^{1/2} \quad \text{(Equation 10)}$$

With:

$$N_p = \frac{\rho_m}{\rho_l}$$

Where:

$Lbrk$ : the hypothetical jet breakup length could be calculated

$\rho_m$ : molten corium density (kg/m<sup>3</sup>) sampled from density

$\rho_l$ : water pool density @ (1 bar) saturation 958.63 (kg/m<sup>3</sup>)

$C \sim 10$ : a constant value of 10 is used in Reference 3. However a uniform distribution between 7 and 13 has been adopted in this analysis based on Reference 2.

Results of the Revised Analysis:

This revision resulted in the increase of the containment failure probability by 45 percent from 5E-3 to 7.25E-3. The total frequency of the accident sequences affected by this change is approximately 4.E-10/ yr. These sequences are not part of the large release frequency (LRF); therefore, this revision has no impact on the risk metrics reported in the FSAR Chapter 19.

The following figures provide initial and revised results for the stated parameters:

- Figure 19-334-4—Premixed Mass Lateral Leak (kg)
- Figure 19-334-5—Premixed Mass Central Leak (kg)
- Figure 19-334-6—Pit Wall Pressure from Lateral Leak (kg)
- Figure 19-334-7—Pit Wall Pressure from Central Leak (kg)

## 2. Benchmark Of The Blast Correlation With NUREG CR-6849

To benchmark the blast correlation model the results from the base case and sensitivity studies from Reference 6 were analyzed. This benchmark was performed by estimating the premixed mass (not provided in Reference 6) and varying the efficiency until the reported loads were matched.

The results of the benchmarking show the following:

- The blast correlation is capable of reproducing the predicted pressure peaks presented in Reference 6. This implies that the use of this correlation is appropriate in the context of a probabilistic model of blast loads.
- The durations predicted by the blast correlation appear to match quite closely with the width of the first peak on the individual load versus time curves presented in Reference 6. However, the blast correlation assumes a theoretical triangular load shape which differs from the shape of the transient load curves calculated in Reference 6. As a result the blast correlation tends to predict lower cumulative impulses calculated than Reference 6.
- Reference 6 predicts considerable reflected pressure peaks which contribute considerably to the final impulse load values presented. The usual application of the blast correlation does not account for the reflected peaks. The predicted magnitude of the reflected peaks in the Reference 6 analysis may arise from numerical/nodalization aspects of the modeling rather than representing expected physical behavior.

## 3. Efficiency Range Used in the Uncertainty Analysis

In the benchmarking study the terms “explosion efficiency” and “conversion ratio” are equivalent. The conversion ratio is the ratio of mechanical energy produced by the explosion to the available thermal energy.

The efficiency range used in the uncertainty analysis is between 0.15% and 20%. This range is based on a literature review (References 7 and 8) and justified by the initial conditions of steam explosion in the U.S. EPR plant. Furthermore, in the benchmarking the blast correlation used in the uncertainty analysis it was noted that efficiencies around 10-12% reproduced the best estimate pressure loads from Reference 6 and the best estimate analysis of the U.S. EPR design.

Finally, the loads produced in the uncertainty analysis cover pressures loads up to 150 MPa for the wall and up to 41 MPa for the melt plug. These loads are considered high enough to produce a bounding pit failure probability.

In conclusion, the efficiency range selected is based on independent analyses and adequate for the initial conditions considered, the efficiency used to match the base case from Reference 6 is within this range and any variation of the efficiency upper bound would not impact the pit failure probability or the LRF.

### **Response to Question 19-334, Part b:**

#### **Accounting for In-Vessel Event Progression Uncertainties in the U.S. EPR Design**

The U.S. EPR strategy for temporary melt retention prior to relocation to the corium spreading room significantly reduces the likelihood for late corium relocations (such as after failure of the melt plug and gate) from the RPV and the ex-vessel steam explosion threat to containment integrity. Temporary melt retention is provided by sacrificial and protective layers in the reactor cavity. The sacrificial layer is intended to delay melt progression in the vertical direction and contact with the melt gate until effectively the entire corium inventory has been released from the RPV.

Tolerance to such event progression uncertainties is indicative of the U.S. EPR “self-adjusting” characteristic of molten corium-to-concrete interaction (MCCI) in the reactor cavity. The length of the temporary retention phase is driven by the release rate of corium from the RPV. There is a defined amount of concrete that is ablated during MCCI. The energy required for MCCI comes from the decay heat in the melt. For fast releases of corium from the RPV, there is an abundance of energy and MCCI proceeds quickly. For slow releases of corium from the RPV, the decreased amount of energy in the melt reaching the reactor cavity causes MCCI to proceed at a slower rate. This leads to a longer retention phase, allowing more of the melt to accumulate in the reactor cavity. The energy balance gives the melt retention phase a self-adjusting characteristic that decouples the spreading process from the uncertainties of the in-vessel phase of the severe accident.

#### **In-Vessel Melt Progression Considerations**

To assess the potential consequences of late relocations, the physical processes and uncertainties that could lead to such a situation must be considered. Much of what is understood about in-vessel severe accident progression in a large pressurized water reactor comes from the Three Mile Island Unit 2 (TMI-2) accident (Reference 10). Approximately 25 tons of core material relocated from the core region into the lower plenum at TMI-2. During the early phases of the severe accident, such as that following the onset of fuel melting, molten corium pooled on top of the lower core support plate. Coolant, either resident in the lower regions of the RPV or being forced via reactor coolant pumps, oxidized and cooled much of this fuel, allowing crusts to form both within and on top of the lower core support plate. These crusts prevented the corium from flowing directly to the lower plenum. The melt accumulated and flowed to the periphery, contacting and fatiguing the baffle and former plates and eventually leaking through the outer edges of the lower core support plate.

The progression is expected to be similar in that an oxidic crust is expected to form in and on the lower core support plate in the U.S. EPR. Corium will flow toward the periphery of the core, contacting the heavy reflector. Because of the large mass, and correspondingly high heat capacity, the heavy reflector and lower support plate act as a temporary internal crucible, retaining the core within its boundary. It is expected that this intermediate molten pool will already contain a large fraction of the core. Melt-through of the heavy reflector, driven by natural convection, is expected to occur in the upper region of the molten pool. During melt relocation into the lower plenum, the continued heating within the core coupled with the out-flowing melt is expected to widen the initial hole, allowing more core melt to relocate.

While much of the core material is expected to be in the lower plenum when the lower head fails, small local pools of corium may still reside on intact portions of the lower core support plate. The U.S. EPR temporary melt retention feature was designed for this in-vessel event progression uncertainty. The lower core support plate will continue to fatigue from direct contact with corium and from the thermal radiation generated from the corium pool in the reactor cavity. The combined thermal and mechanical loads are expected to relieve the remaining corium pools through either local or global failure of the lower core support plate prior to melt plug failure. The breach of the reactor pressure vessel and local lower core support plate failures can potentially relieve the "crucible-effect," allowing for some refreezing, particularly fuel and cladding oxides which have relatively high liquidus temperatures. As with the temporary melt retention concept, the state of any remaining corium pools is self-adjusting: the longer the lower core plate remains intact, the more likely that corium cools and refreezes, further reducing the likelihood of a late relocation of molten corium entering a wet cavity and transfer channel.

### **Assessment of Steam Explosion Potential from Late Relocations**

A possible scenario in the U.S. EPR ex-vessel severe accident mitigation strategy is an early failure of the melt plug. In this case, late melt discharge into the reactor cavity and transfer channel may trigger a steam explosion.

Late corium relocations from the U.S. EPR core region falling into a flooded transfer channel would not experience optimal conditions for a violent steam explosion. The main reason is that the water residing in the spreading room and transfer channel quickly saturates and boils off. The presence of nucleate boiling maintains a stable vapor film around the molten fuel, which significantly reduces the potential for fragmentation. This situation reflects the condition in which the interfacial temperature between the molten material and water is lower than the material melting temperature.

The likely trigger mechanism will be the impact of the pour onto the surface of the encrusted corium already in the transfer channel from the initial relocation. As with having saturated water, a relatively soft surface like corium will dampen the trigger force. In addition, the stability of the corium crusts will not likely hold a significant pour and will likely absorb the melt, preventing the kind of fragmentation necessary for steam explosion.

### **Ex-vessel Steam Explosion Evaluation for the U.S. EPR**

For the reasons cited above, a bounding ex-vessel steam explosion evaluation was performed as originally described in AREVA's RAI 133, Supplement 6, Response to Question 19-230, involving an induced hot leg rupture with the reactor coolant system at high pressure, allowing

cool accumulator water to enter the reactor cavity. The key assumptions incorporated in that analysis, including fuel and water mass and temperature, confined geometry, conversion ratio, lead to a more challenging steam explosion condition than can be practically envisioned with a late relocation scenario.

A qualitative review of the design of the reactor cavity, transfer channel and spreading area resulted in the conclusion that the impact of a steam explosion in the reactor cavity would bound any impact of a steam explosion in the transfer channel. However, due to the limited capacity of the spreading area the containment event tree (CET) will be revised to include a probability of spreading area failure given a late relocation occurring along with the conditions for a steam explosion in the spreading area.

The U.S. EPR Probabilistic Risk Assessment (PRA) and U.S. EPR FSAR Tier 2, Chapter 19 will incorporate the revised assumptions on spreading area steam explosion as part of the PRA update being performed in response to RAI 289, Question 19-239. U.S. EPR FSAR Tier 2, Chapter 19 will be revised to reflect the new assumptions, and will be included with the Response to RAI 289, Question 19-239.

#### **References to Question 19-334:**

1. Comparative Review of FCI Computer Models Used in the OECD-SERENA Program, Paper 5087 Proceedings of ICAPP '05 Seoul, KOREA, May 15-19, 2005 (2005).
2. K.Moriyama and al. "Evaluation of Containment Failure Probability by Ex-vessel steam explosion in Japanese LWR plants", Journal of Nuclear Science and Technology, Vol 43, No. 7, p. 774-784 (2006).
3. K.Moriyama and al. "Coarse break-up of a stream of oxide and steel melt in a water pool, JAERI-Research 2005-17, (2005).
4. K.Moriyama and al. "A simple evaluation method of the molten fuel amount in a premixing region of fuel-coolant interaction", Journal of Nuclear Science and Technology, Vol 39, No. 1, p. 53-58 (2002).
5. OECD Research Programme On Fuel-Coolant Interaction Steam Explosion Resolution For Nuclear Applications – SERENA, Final Report NEA/CSNI/R(2007)11, (2006)
6. NUREG/CR-6849 "Analysis of In-Vessel Retention and Ex-Vessel Fuel Coolant Interaction for AP1000"., ERI/NRC-04-201. August 2004
7. Failure From In- Vessel Steam Explosions," NUREG-1116 (SERG-1 Report), June 1985.
8. USNRC, "A Review of the Current Understanding of the Potential for Containment FSAR Impact:
9. USNRC, "A Re-assessment of the Potential for an Alpha-Mode Containment Failure and a Review of the Current Understanding of Broader Fuel Coolant Interaction Issues," NUREG-1524, August 1996.

10. W. Cronenberg, E. L. Tolman, "Thermal Interaction of Core Melt Debris with Three Mile Island Unit 2 Vessel Components," Nuclear Technology, Vol. 87, Aug. 1989.

**FSAR Impact:**

The U.S. EPR FSAR will not be changed as a result of this question.

**Table 19-334-1—Summary of Failure Probabilities:**

	Probability of failure given triggering	Probability of failure with [ ] probability of triggering	Combined failure probability [ ]
Pit Wall	4.E-05	3.E-05	7.2E-03 <sup>1</sup>
Melt Plug	1.7E-01	1.E-01	

**Notes:**

1. Note that in the initial analysis the containment failure probability value used was rounded up from 2E-3 to 5E-3. The best estimate resulted in a failure probability of 2E-3 and the uncertainty analysis resulted in a failure probability of 9E-4.
2. The conditional probabilities of lateral versus central leak of the RPV have been described in the RAI 133, Supplement 6, Response to Question 19-230.

**Figure 19-334-1—Jet Velocity Distribution**



**Figure 19-334-2—Droplet Size Distribution**



**Figure 19-334-3—Void Fraction Distribution**

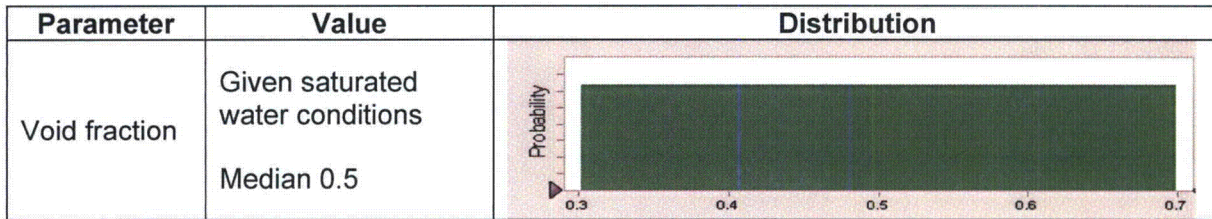
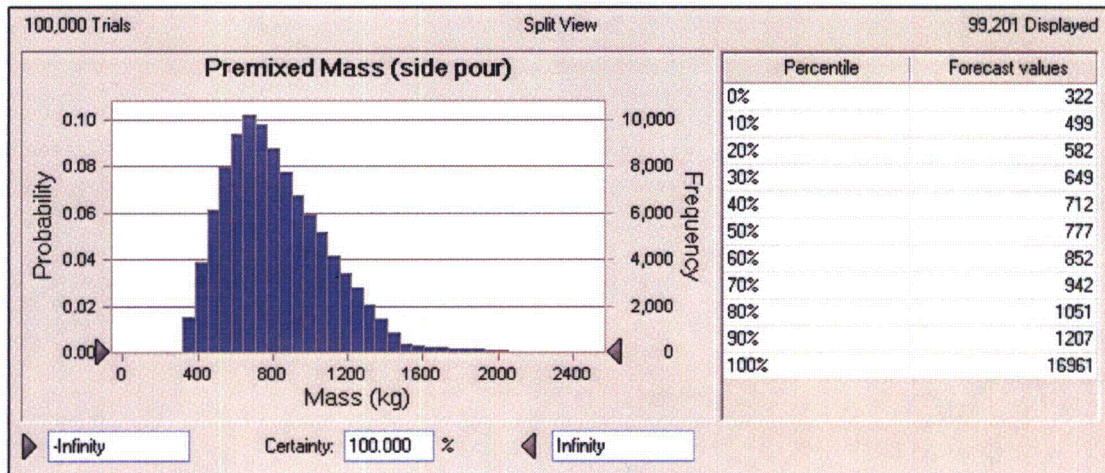


**Figure 19-334-4—Premixed Mass Lateral Leak (kg)**

**Initial Analysis**



**Revised Analysis**

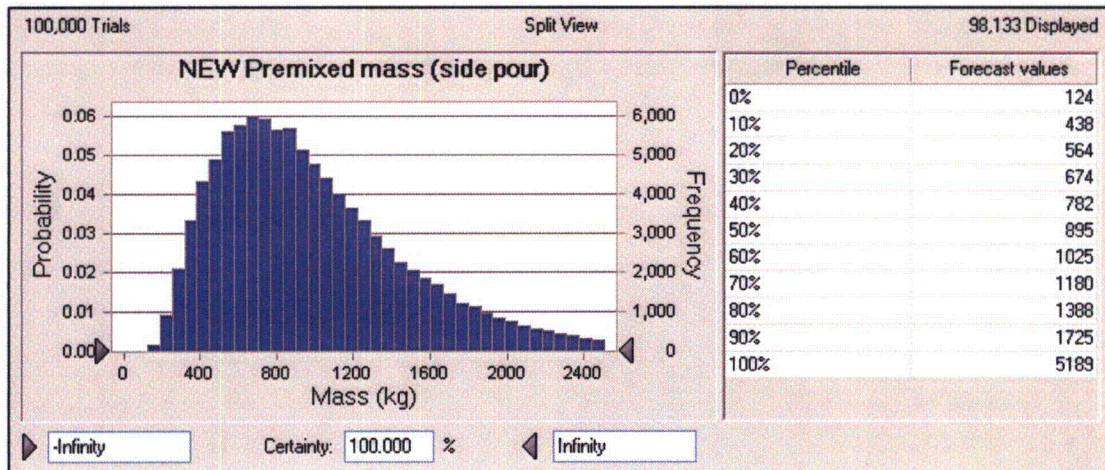
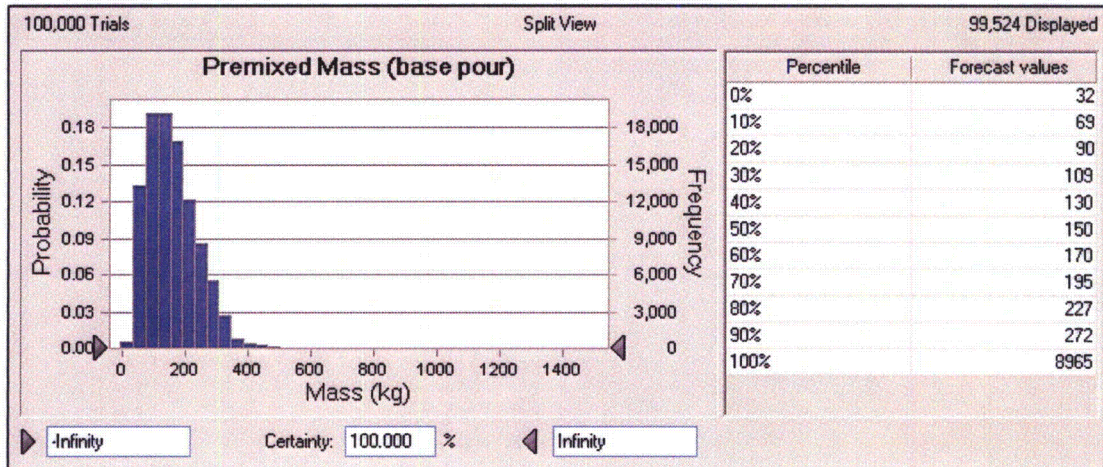


**Figure 19-334-5—Premixed Mass Central Leak (kg)**

**Initial Analysis:**



**Revised Analysis:**

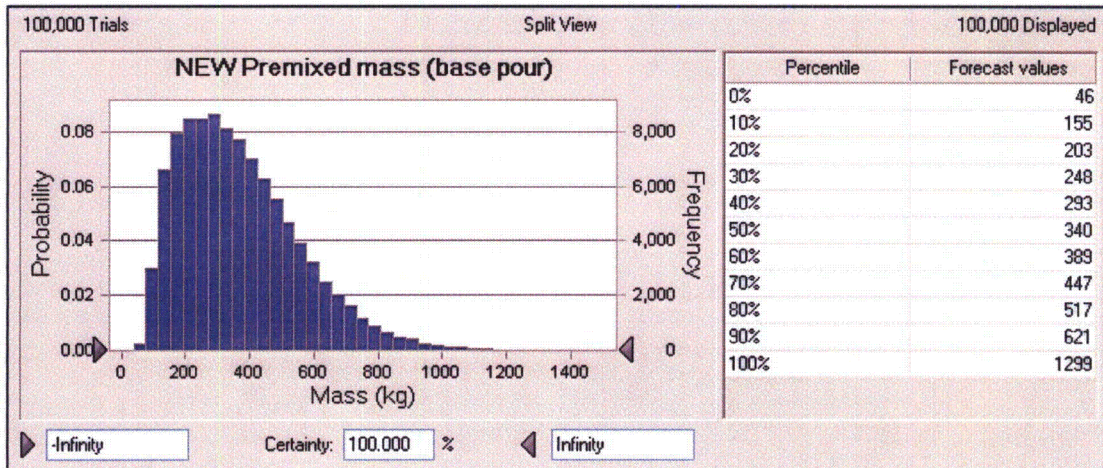
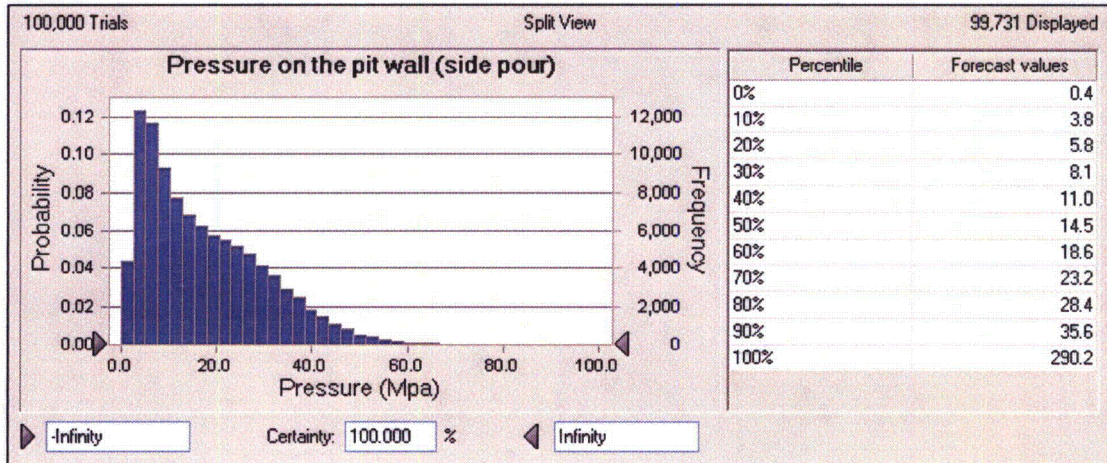


**Figure 19-334-6—Pit Wall Pressure from Lateral Leak (MPa)**

**Initial Analysis:**



**Revised Analysis:**

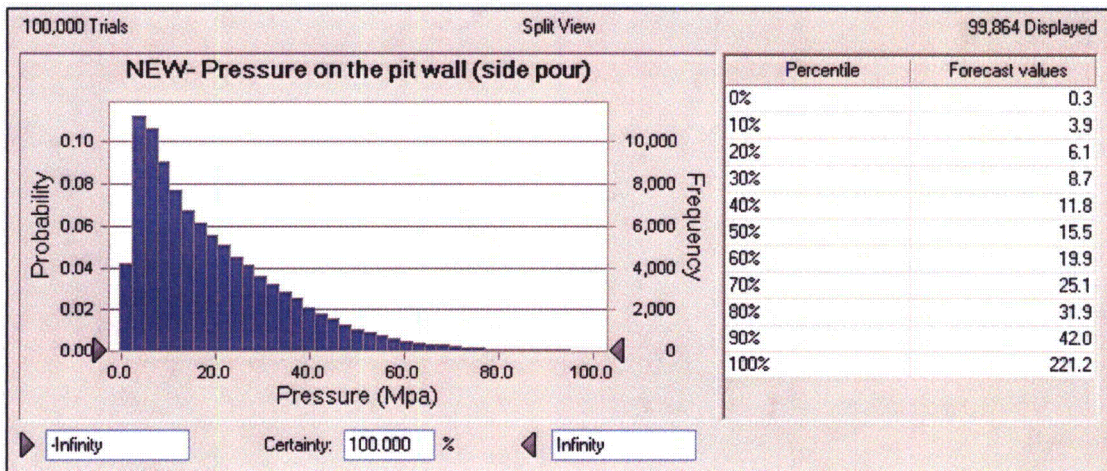
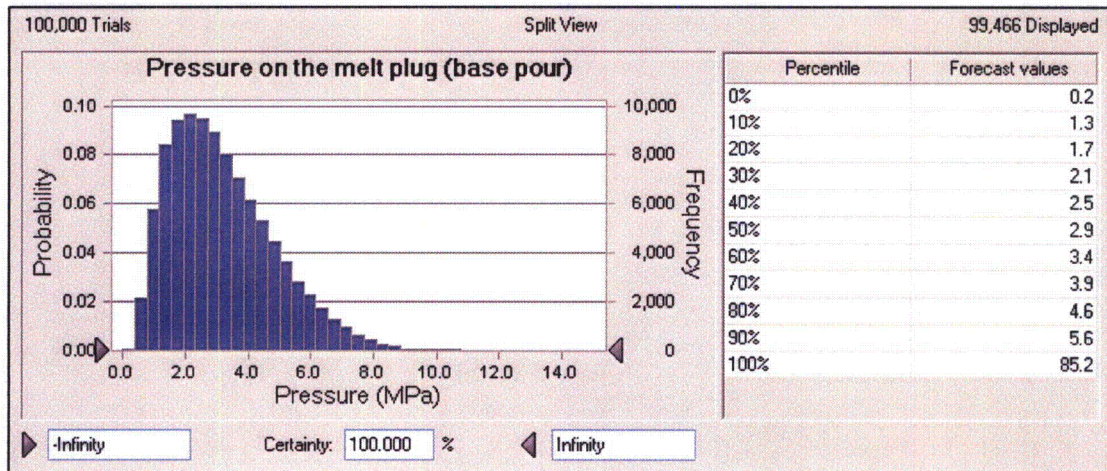
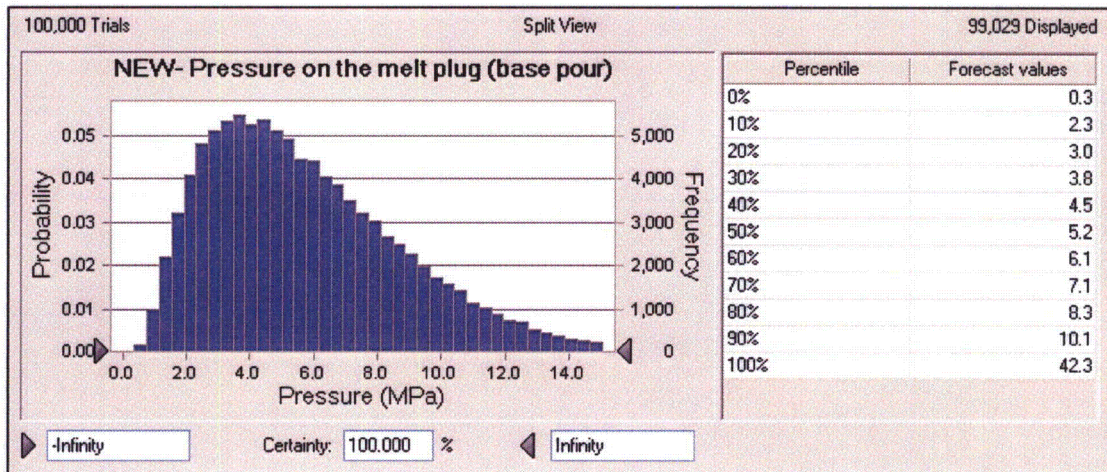


**Figure 19-334-7—Pit Wall Pressure from Central Leak (MPa)**

**Initial Analysis:**



**Revised Analysis:**



**Question 19-335:**

## OPEN ITEM

Follow-up to RAI 133, Question 19-233

This was a follow-up to Question 19-84e. The response shows a calculation of likelihood of multiple Steam Generator Tube Rupture (SGTR) using a Poisson distribution due to random flaws in the tubes under creep-induced conditions. The analysis does not treat/consider the potential implication of failure propagation due to the continued heat-up of the steam generator tubes, after the initial tube failure. Natural circulation and steam generator tube heat-up is expected to continue well beyond the failure of a single tube. Therefore, the analysis of the calculated failure likelihoods is incomplete.

The calculated fission product releases to the environment for the single and multiple tube failure based on MAAP results are low. In comparison to the recent NRC MELCOR calculations for a single double-ended induced-SGTR scenario, the MAAP results cited in AREVA response, are about 50% too low. One reason is the termination of MAAP calculations after 24 hours, thus limiting the releases due to revaporization. These differences are significant and need to be reconciled.

- a. Please revise the analysis to reflect the potential impact of continued heatup of the steam generator tubes, and determine at what level of failure (number of tubes), RCS depressurization occurs, terminating additional tube failures.
- b. Please extend the present source term calculations to at least 48 hours, and report the impact on fission product releases and severe accident risk for U.S. EPR.

**Response to Question 19-335****Response to Question 19-335(a):**

The analysis presented in RAI 133, Supplement 2, Response to Question 19-233 has been extended to investigate the continued heatup of the steam generator (SG) tubes following the initial rupture. This analysis focuses on the potential for multiple tube failures as a result of this heatup.

An SG experiencing creep induced tube rupture will continue to heat up after the initial rupture, with a sustained high differential pressure across the tubes. The heat up of the tubes is driven by the enhanced flow of hot gases through the existing SG break.

A number of modular accident analysis program (MAAP) runs have been performed with an increased number of SG tube failures. Figure 19-335-1 shows the primary system pressure for a single and multiple SGTRs; 1, 10, 20, 30, 50 and 100. Figure 19-335-2 shows the maximum wall temperature for SG tubes as a function of time after a given number of tube ruptures.

After the initial heat up, the drop in the wall temperature of the tubes is immediate and significant for greater than or equal to 20 ruptured tubes, indicating that the tubes are adequately cooled down, therefore precluding additional ruptures.

Figures 19-335-1 and 19-335-2 show that adequate depressurization and cooldown of the SG tubes is reached with a break area equivalent to the rupture of a maximum of 20 tubes, assuming that no induced hot leg rupture (IHLR) occurs. If IHLR occurs at any time after the initial tube rupture, additional SGTRs will be precluded due to the rapid and complete depressurization of the primary system leading to a stress relief across the tubes and their cool down.

#### Evaluation of Multiple Steam Generator Tube Failures Timings:

A cascade of multiple SG tube failures could be arrested as a result of:

- The occurrence of IHLR at anytime during the transient scenario.
- A rapid rupture of a sufficient number of SG tubes to achieve adequate cool down and pressure relief across the tubes.

For high pressure accident scenarios, the likelihood of the creep IHLR occurrence is significantly higher than the creep induced steam generator tube rupture. The phenomenon of IHLR has been extensively discussed in RAI 6, Supplement 1, Response to Question 19-079 and the probabilities of piping failure due to creep induced ruptures have been summarized in Table 19-79-6. The occurrence of IHLR leads to an immediate depressurization of the primary system, subsequently precluding any further steam generator tube ruptures.

The timing of IHLR relative to additional SG tube ruptures has been analyzed for 1, 10 and 20 tube ruptures. These cases have been selected based on the earlier conclusion that multiple SGTRs involving more than 20 tubes were not credible because of the rapid cooldown of the tubes.

The analysis is focused on the timeframe following the first tube rupture. Using the temperature and pressure histories after the initial failure from MAAP and the Larson-Miller correlation (Equations 1 and 2), the timing of additional steam SGTRs was evaluated.

$$LMP = T * (A + B * \ln(tr)) * 10^{-3} \quad \text{(Equation 1)}$$

$$\ln(\sigma) = m_{fi} * LMP + b_{fi} \quad \text{(Equation 2)}$$

With:

$LMP$  : Larson-Miller parameter

$T$  : Wall Temperature (K)

$tr$  : rupture time (sec)

$A, B$  are fitting parameters for Inconel 690 and they are 29.5 and 0.782 respectively

$$\sigma = \frac{\Delta P * r}{x}$$

: stress (Pa)

$\Delta P$  : pressure difference across the SG tube wall (Pa)

$r$  : SG tube radius (m)

$x$  : SG wall thickness (m)

$m_{fit}, b_{fit}$  are fitting parameters for Inconel 690 and they are -0.1777 and 25.4198 respectively

The rupture times calculated and shown in Figure 19-335-3 are from the point where the first rupture is predicted forward. The X-axis represents the real time in hours while the Y-axis represents the theoretical time of tube ruptures (initial and subsequent ruptures) calculated using the Larson Miller correlation. Note that a linear plot indicating that the calculated rupture time is equal to the real time is shown in Figure 19-335-3. The intersection of this linear plot and the calculated rupture time indicates the occurrence of a predicted rupture. The times of hot leg ruptures predicted by MAAP are also shown in the same figure. They are indicated by dots along the linear plot and their values shall be read on the X-axis since they represent real events. The following was concluded from the plots:

- Case of one induced SGTR (Green plot on Figure 19-335-3): Additional failures are predicted within a few minutes of the initial tube failure. The hot leg rupture is predicted to occur much later than the next tube failures; therefore, it cannot be credited to stop further tube ruptures.
- Case of 10 induced SGTR (Blue plot on Figure 19-335-3): No additional failure time is calculated prior to the occurrence of hot leg rupture. The pressure and temperature values at any given time after the initial rupture are not sufficient to sustain a cascade of additional tube failures.
- Case of 20 induced SGTR (Magenta plot on Figure 19-335-3): In this case, the hot leg rupture is predicted to occur before any additional tube rupture thus terminating the cascade of tube ruptures.

Note that the additional tube rupture shown in Figure 19-335-3 for the case of 20 induced SGTR is a result of not modeling the IHLR when predicted by MAAP. If the IHLR was modeled, the pressure and temperature profiles would have been lower and thus no additional ruptures would have been calculated. The purpose of preventing the IHLR was to model harsher conditions on the SG tubes.

It can be concluded from these results that the maximum number of SGTRs from the heatup initiated by the first rupture will be no greater than 10 tubes.

Table 19-335-1 summarizes the source term resulting from a single tube rupture and 10 tube ruptures at 48 hours. Based on the conclusions of this analysis, these two cases are considered to adequately bound the range of expected multiple SGTRs.

It is noted that the MAAP runs used in this analysis are based on the latest revision of the U.S. EPR MAAP model and the results are slightly different from those presented in the RAI 133 Supplement 2, Response to Question 19-233.

**Response to Question 19-335(b):**

Figure 19-335-4 shows the original MAAP4 results of fission product releases for the single induced-SGTR scenario extended out to 48 hours. These releases are approximately half of the values determined by the NRC MELCOR analysis with no appreciable change in the time period from 24 to 48 hours for the volatile fission products, data provided in Table 19-335-2.

For the first 24 hours, the differences in the releases were traced to the timing of the occurrence of the steam generator tube rupture. For MELCOR (based on the NRC provided information for the MELCOR analysis), the rupture occurs prior to significant core degradation (release of fission products into the RCS). In other words, the SGTR was assumed to be the initiating event.

In the reported MAAP analysis, the SGTR is assumed to occur after significant core degradation (after significant release of fission products to the RCS), allowing for time for significant plate-out of fission products on the walls of the RCS to occur. This delay in SGTR in the MAAP analysis allows for a reduction in the availability of fission products to be released (i.e., in the MAAP analysis, the SGTR occurs when there is less airborne fission products in the RCS). It should be noted that we are in the process of revising the source term documentation including a revision to the MAAP model. Preliminary results of the new analysis show substantial earlier SGTR failure, i.e., prior to major fission product release from the fuel. We are also incorporating the provision for SGTR to occur as an initiating event, in addition to previous scenario of only a thermal-induced SGTR.

For the response to this particular question, and to mimic the MELCOR analysis as close as possible, an early SGTR failure was modeled in MAAP by a forcing function to create a steam generator tube rupture at 3000 seconds. For at least the first 24 hours, the revised MAAP4 model predicted fission product releases are well within the NRC MELCOR calculated values; see Table 19-335-3. For the next 24 hours, out to 48 hours, only the noble gases continued to agree, confirming that the volume versus break flow is similar between the MELCOR and MAAP4 models. For the MAAP4 model, no appreciable change in volatile fission product release was noted for the subsequent time period (24 to 48 hours); see Figure 19-335-5.

This lack of subsequent release can be traced to the relocation of the deposited fission products out of the primary circuit apparent in the MAAP4 calculation (see Figure 19-335-6), resulting in a relatively low concentration of volatile fission products (e.g., cesium and iodine) in the primary system; and, ultimately, a lower decay heat.

A similar reduction can be noted in the MELCOR calculations for CsI and Te, see Figure 19-335-7, but not for Cs, a species that can be either in the form of CsOH or Cs<sub>2</sub>MoO<sub>4</sub>. Assuming that the gas flow through the failed tube is similar (based on the noble gas release) between MAAP and MELCOR, the differences for Iodine and Te (which have similar vapor pressure calculations) are most probably the result of higher gas temperatures being predicted by MAAP within the RCS, relocating these fission products to the containment via the small break.

Further review of the NRC MELCOR's result for RCS retention during the first 24 hours, Figure 19-335-7, reveals that the Cs within the RCS deposits extremely rapidly and remains on the RCS surfaces as opposed to either Iodine or Te, as noted by the lack of a dip in the fission product fraction. Again, this trend is significantly different than that predicted by MAAP4 (see Figure 19-335-6). Within MAAP4, approximately 30% of the Cs is retained within the Primary System with almost 60% being predicted to be retained by MELCOR. This prediction agrees well with those discussed in (Reference 1) Jason Schaperow's paper "Investigation of a Steam Generator Tube Rupture Sequence Using VICTORIA," which shows MELCOR having approximately 80% retention of Cs in the RCS as opposed to MAAP's 32 % retention for Cs.

For both MAAP and MELCOR after the initial spike of fission products in the primary circuit, the RCS continues to depressurize, transferring fission products from the RCS to the containment via the 2" line break and to the environment via the steam generator tube rupture. This removal is from two sources – suspended (airborne) and vaporization of deposited fission products on the RCS walls (including the steam generator tubes). For suspended fission products, the removal is via the typical flow paradigm. For deposited material, the removal involves the vaporization and subsequent transport of fission products from the primary system.

For MELCOR, the condensation and evaporation from the heat structures (RCS Surfaces) are controlled by the vapor pressure of the individual fission product classes. This is based on the statement in Section 2.5.2 of the MELCOR's RN Package Reference Manual:

In addition to being used to determine the amount of each material class present as aerosol and as fission product vapor, the vapor pressure is used in the model for condensation and evaporation to determine the saturation concentrations,  $C_i^s$ , calculated from the perfect gas law,...

An analogous paradigm also exists within MAAP. Therefore the rate of vaporization off of the primary system heat structure calculated by MAAP4 and MELCOR is dependent upon the vapor pressure algorithm within the two codes, which is based on the temperature of the surrounding gas and structure. In general, MELCOR and MAAP share almost the exact parameters for the algorithm used in determining the vapor pressure, specifically for Class 16 (CsI) in MELCOR and Class 2 (iodine) in MAAP. The most significant difference is that MELCOR contains a new class,  $Cs_2MoO_4$ , which is not available in MAAP. This is a new class developed post release of MELCOR 1.8.6 and has much lower vapor pressure than CsOH. This new class is modeled via the input file for MELCOR. This input file was not available for review, and thus could not be compared to the values of vapor pressure for CsOH used in the MAAP cases supporting the US EPR SGTR analysis.

In retrospect, the lack of additional release after 24 hours in the MAAP4 models was traced to the small amount of fission product plate-out that MAAP4 is predicting for the primary circuit; see Figure 19-335-6. For Cs, the values shown in Figure 19-335-6 are less than a quarter of the values predicted by MELCOR, Figure 19-335-7. For Te, the values are only a fraction of the values reported by MELCOR. In general, it appears the MELCOR is predicting sufficiently less revaporization of material within the primary circuit than MAAP4 (and associated decay heat) during the initial 24 hours.

Subsequent to 24 hours, it is these deposited volatile fission products with their increased decay heat that constitute the principle increase in the non-Noble Gas source terms through the failed

steam generator tubes as a result of revaporization of deposited material on the RCS surfaces as predicted by MELCOR.

The revaporization phenomenon of Cs including the high concentration of  $Cs_2MoO_4$  is driven by high temperatures described in Reference 2, coming from the decay heat of the deposited fission products on the RCS surfaces. From the MAAP input deck, CsOH contains about 3 % of the decay energy; therefore, MAAP predicts only about 0.9% (30% retention of the Cs in the primary system multiplied by 3% power fraction) of decay power is associated with the CsOH remaining on the RCS surfaces after the initial release. Within MELCOR, this percentage increases to almost 2% (assuming the same power fraction with an 80% retention) of the decay power, a factor of more than twice. Thus, MAAP4 does not predict the high temperatures in the RCS necessary for revaporization of Cs (i.e., 400 to 500°C per Reference 2) after the initial 24 hours as a result of lower mass of fission products (and associated decay heat) remaining on the RCS surfaces.

In addition, the area over which the deposition occurred may be dramatically different between the two codes. MAAP inherently allows for natural circulation within the hot leg; however, MELCOR does not. Therefore, to allow for natural circulation, the MELCOR user must divide the RCS piping (top half and bottom of the hot leg) in half with one half being the flow to the steam generator and the other half being the return. The end result is that the deposition area associated with the MELCOR model may be significantly smaller than that available in the MAAP model, concentrating the deposited material in a smaller area.

Additionally, plant operators for beyond 24 hours will be responding to event consequences through Severe Accident Management Guidelines (SAMG) as outlined in Section 3.10 of the Technical Report, "The Operating Strategies for Severe Accident Methodology for the U.S. EPR," and should have recovered at least partial operation of the plant (including containment cooling, which was conservatively neglected in these analyses). Several strategies for controlling the release of fission products through a failed steam generator tube can be envisioned and will be evaluated through AREVA's Operating Strategies for Severe Accidents (OSSA), used in the development of U.S. EPR SAMGs.

Given that the results from the revised MAAP4 analysis are in strong agreement with MELCOR for the first 24 hours (assuming the early MELCOR predicted time of SGTR) and the uncertainty regarding the event progression beyond 24 hours, specifically with regards to the deposition, and the revaporization of Cs and I in the RCS piping and steam generators (which occurs at relatively high temperatures within the primary circuit); it is concluded that MAAP4 is providing adequate release estimates for the postulated SGTR.

#### **RAI References:**

1. Bixler, N. E., C. M. Erickson, and J. H. Schaperow, "Investigation of a Steam Generator Tube Rupture Sequence using VICTORIA"
2. Herranz, L. E., et.al., "Progress in Understanding Key Aerosol Issues"
3. ANP-10314 R0, "The Operating Strategies for Severe Accidents Methodology for the U.S. EPR", Technical Report.

**FSAR Impact:**

The U.S. EPR FSAR will not be changed as a result of this question.

**Table 19-335-1—Source Term from a Single and Multiple Steam Generator Tube Ruptures**

Source Term (at 48 hours)	XE/KR Group 1	I Group 2	Cs Group 6	Te (Sb) Group 10	Sr Group 4	Ru Group 5	La Group 8	Ce Group 9	Ba Group 7
1 induced SGTR	16.3%	8.4%	8.6%	13.5%	1.3%	10%	0.05%	0.2%	6%
10 induced SGTR	69.5%	40.4%	44.1%	70.3%	9.7%	47%	0.3%	1.4%	28.3%
Average source term (1, 10) induced SGTR	43%	24.4%	26.35%	41.9%	5.5%	28.5%	0.2%	0.8%	17.15%
Increase factor compared to 1 induced SGTR	2.6	2.9	3.1	3.1	4.2	2.9	4.0	4.0	2.9

**Table 19-335-2—NRC MELCOR Radionuclide Release Results:**

	MELCOR	
	24 hours	48 hours
Noble Gases	23.0%	27.0%
I	17.0%	27.0%
Cs	13.0%	17.0%
Te	18.0%	24.5%
Mo	0.6%	0.7%
Ba	0.2%	0.2%
Ru	0.2%	0.2%

**Table 19-335-3—MAAP4 Predicted Fission Product Releases For NRC MELCOR Emulation Model**

TIME Hours	Noble Gases	Iodine	Cs	Te
24.	21.5%	16.8%	14.8%	14.5%
48.	27.6%	16.9%	14.8%	14.5%

**Figure 19-335-1—Primary System Pressure for Multiple Steam Generator Tube Ruptures**

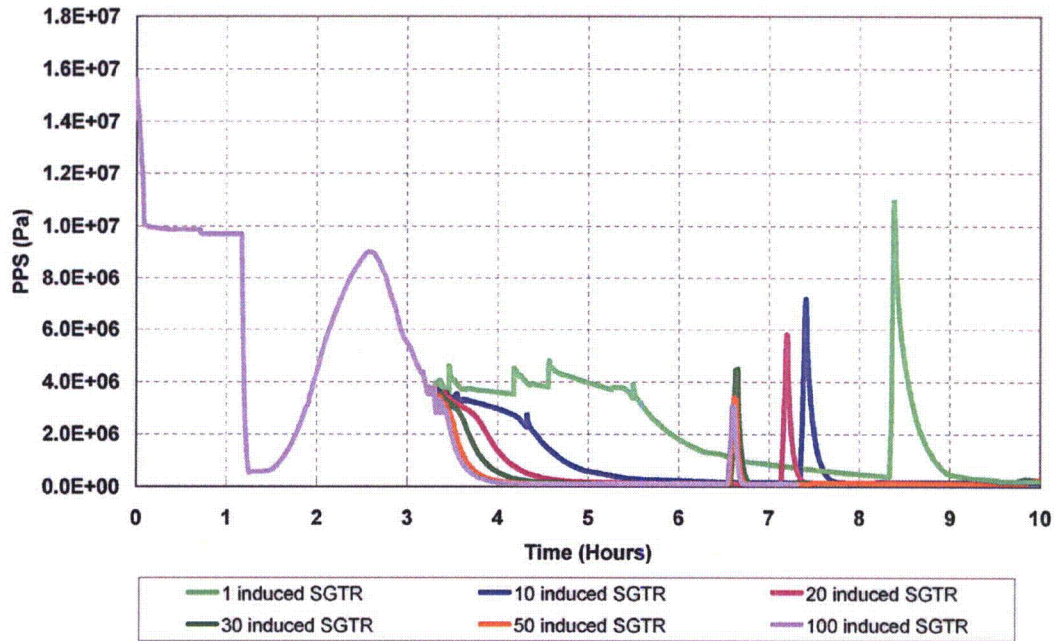


**Figure 19-335-2—Maximum Wall Temperature of Steam Generator Tube for Multiple Ruptures**

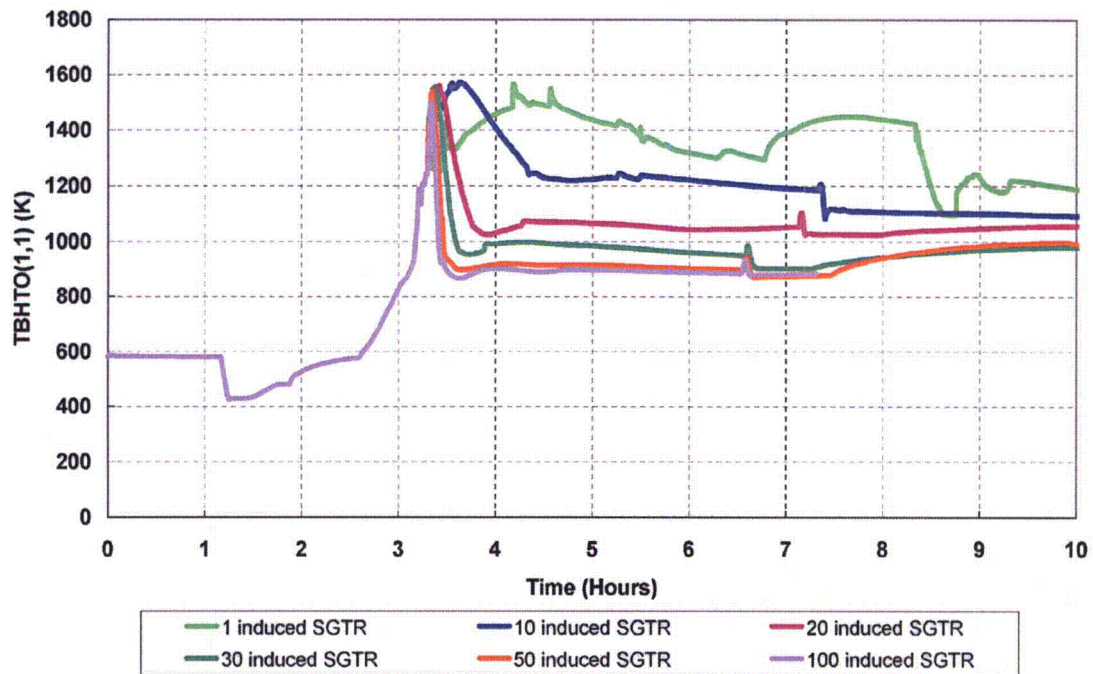


**Figure 19-335-3—Calculated Times of Additional ISGTR following; 1, 10, and 20 Tubes**

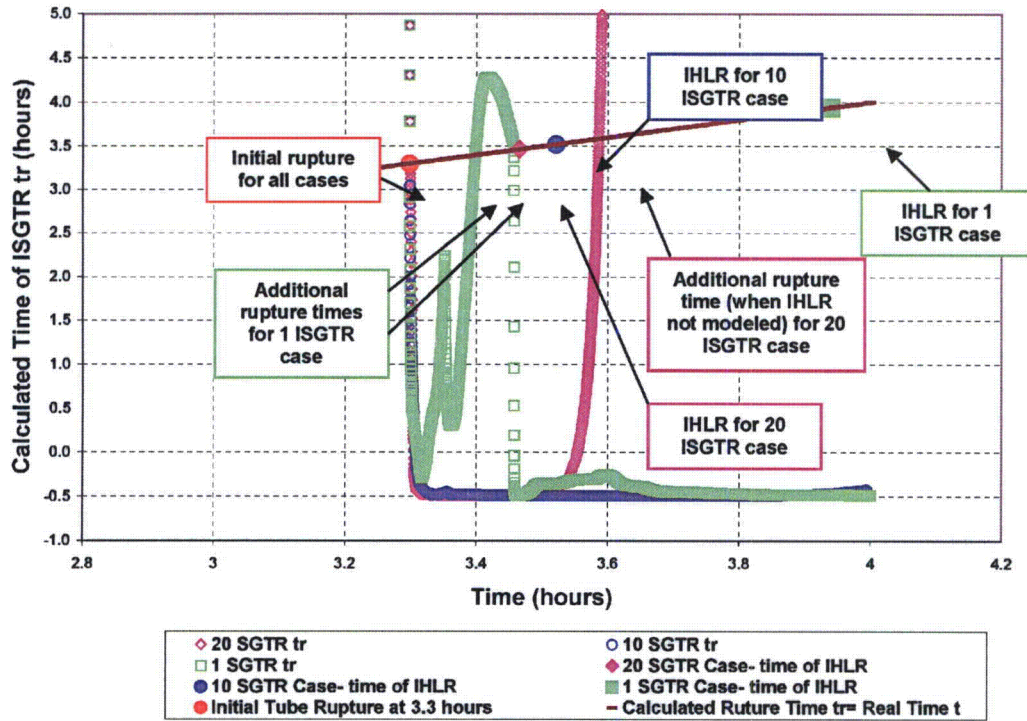


**Figure 19-335-4—Fission Product Releases for 48 Hours Following a Single Induced-SGTR**

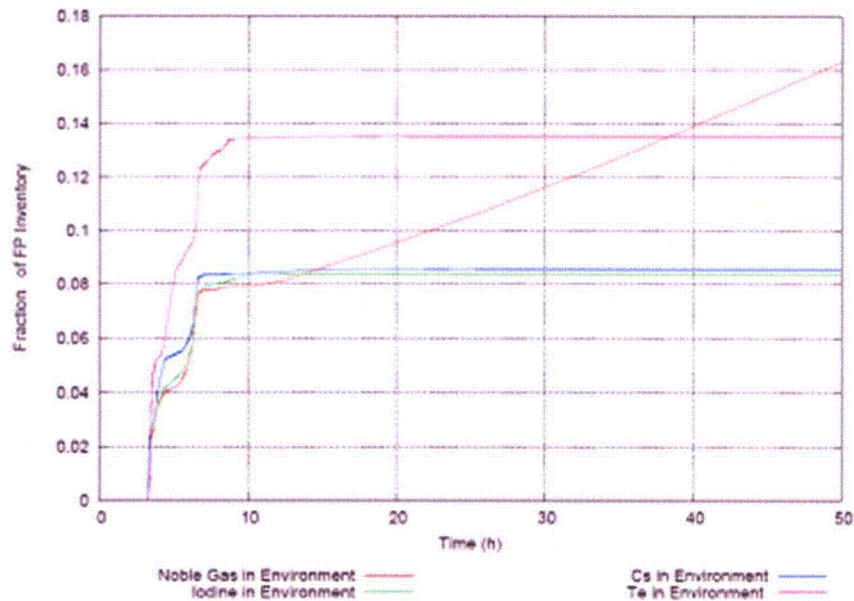


**Figure 19-335-5—MAAP4 Revised Fission Product Releases based on NRC MELCOR Emulation Model**

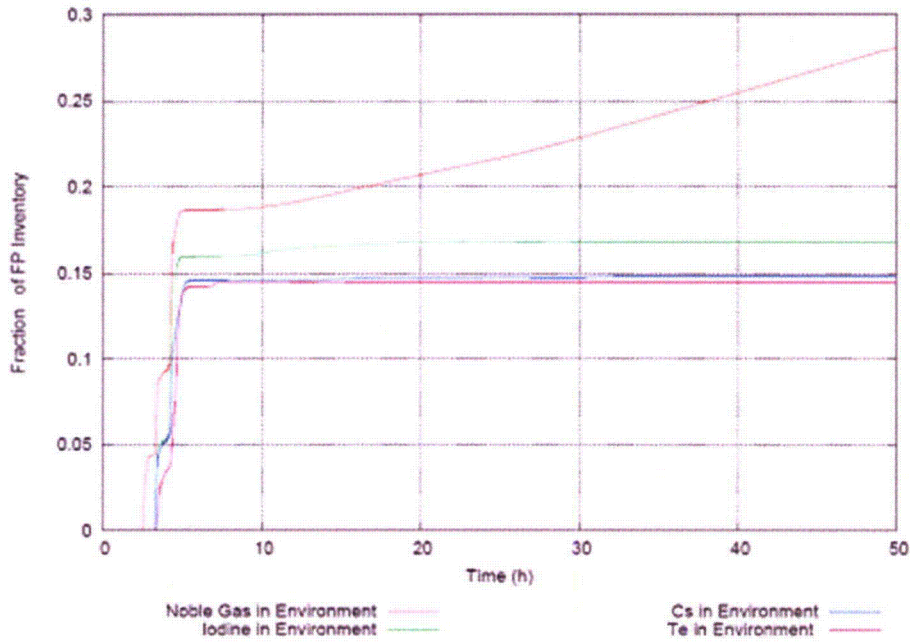


**Figure 19-335-6—MAAP4 Revised Primary Circuit Fission Product Fractions based on NRC MELCOR Emulation Model**

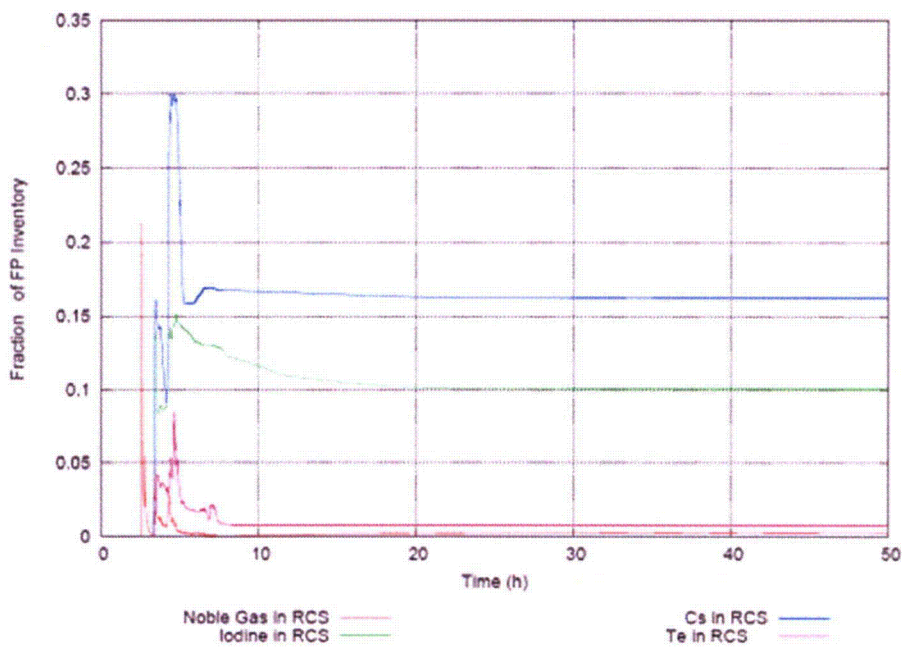


Figure 19-335-7—NRC MELCOR Primary Circuit Fission Product Fractions

